Out-of-Phase Power Divider with Harmonic Suppression

Lulu Bei[1, *], Lei Chen[1], Wenjing Zhao[1], Xulong Zhang[1], Wen Ji[1], and Kai Huang[2]

Abstract—In this paper, a three-layer circuit structure based on double-sided parallel-strip lines (DSPSLs) is proposed to design one out-of-phase power divider (PD) with equal power division and harmonic suppression. This PD, which is composed of four DSPSLs, one middle conductor, and two grounded resistors, features transmission suppression at two specified frequencies and all the even-order harmonics. Closed-form design equations are derived based on the traditional even- and odd-mode methods, and the circuit scattering parameters are also given. Finally, a practical PD operating at 0.92 GHz is designed and fabricated. The measured results show that this PD has equal power division with out of phase, harmonic suppression, good ports matching, and high outputs isolation.

1. INTRODUCTION

Out-of-phase power dividers (PD) [1], which can convert one signal into two-way out-of-phase output signals with equal power division, can be widely used in the balanced circuits and systems, such as push-pull power amplifiers, balanced mixers, and the feeding network of balanced antennas. According to the open literatures, the research about out-of-phase PD can be classified into single-band equal PD [1], single-band PD with arbitrary power division ratio [2], dual-band application [3–5], and single-band PD with complex impedance transformation [6, 7].

On the other hand, the PDs with filtering function or harmonic can be used to suppress unwanted harmonic and can be seen as the combination of the PD and filter. Therefore, lots of circuit structures have been proposed to realize the filtering PDs. For example, two $\lambda/4n$ open stubs, located at the center of the branches, are adopted to design a Wilkinson PD in [8] to realize the nth harmonic suppression. Similarly, four open stubs are used in [9] to realize a filtering balanced-to-unbalanced (BTU) PD. Furthermore, one central loading stub and two side loading stubs are adopted in [10] to realize a Wilkinson PD with filtering function and good isolation performance. The second main method is based on the coupled line or coupling structure. A pair of short circuit anti-coupled lines is adopted in [11] to design a PD operating at 1.8 GHz, and its passband suppression is higher than 20 dB. A coupling structure is used to replace the quarter-wavelength transmission line in [12] to generate two transmission zeros at the passband edges, and the power ratios can also be changed by altering the coupling strength. In addition, a terminated coupled-line structure [13] is adopted to realize a wideband PD with high selectivity, and four transmission zeros are created. Moreover, two inductors are placed at the middle of each branch of the traditional Wilkinson PD to realize the good harmonic suppression [14], too. Apart from the above three methods, other structures and methods, such as the defected ground structure (DGS) [15, 16], microstrip electromagnetic bandgap (EBG) [17, 18], composite right-/left-handed transmission line technology [19], as well as various kinds of resonators [20, 21], can also be used to realize the PD with filtering function because of the slow-wave effect and bandstop performance. However, there is no paper about the three-layer out-of-phase PD with filtering function or harmonic

suppression as we know. The rat-race couplers based on the planar microstrip lines in [22, 23] realize equal power division with filtering function; however, the out-of-phase performance is only limited near the operating frequency. The three-layer out-of-phase PDs [1–7] possess better out-of-phase performance than the rat-race couplers because the double-sided parallel-strip lines (DSPSLs) belong to the balanced transmission lines.

Therefore, a three-layer PD with out-of-phase performance and harmonic suppression is proposed in this paper. This PD, which consists of four DSPSLs, one middle ground, and two grounded resistors, can realize the function of transmission suppression at two specified frequencies, which can be adjusted by changing the electrical lengths of the open stubs. Besides, all the even-order harmonics can also be suppressed because of the isolation network. The circuit structure, even- and odd-mode method, and the theoretical foundation to realize the harmonic suppression are analyzed to design this PD in Section 2. Then, the parameter analysis about impedance Z_3 and Z_4 is discussed in Section 3, and a practical out-of-phase PD operating at 0.92 GHz for the radio frequency identification (RFID) application is fabricated in Section 4. Finally, a conclusion is drawn in Section 5.

2. CIRCUIT STRUCTURE AND DESIGN THEORY

The 3-dimensional circuit structure of the proposed out-of-phase PD with harmonic suppression is depicted in Figure 1. It can be observed that this proposed circuit essentially consists of four DSPSLs on the top and bottom layers, one conductor plane in the middle, and two grounded resistors R_0. Actually, two isolation resistors R_0 can be replaced with one resistor $R_0/2$ on the top (or bottom) layer, and the circuit performance remains unchanged. The electrical length of the DSPSL Z_i ($i = 1, 2, 3$, and 4), which is symmetrical and used for the signal transmission, is θ_i. The middle conductor acts as the common ground, and it can convert the DSPSL Z_4 into one pair of back-to-back microstrip lines. Besides, there is no common ground for the input port and the DSPSLs Z_1, Z_2, and Z_3.

One copper cylinder (CC_1) is adopted to connect one side of two resistors, and the other copper cylinder (CC_2) is used to connect the DSPSL Z_4. It can be seen that the CC_1 is connected to the middle conductor, while the CC_2 is not. Therefore, two resistors R_0 only influence the even-mode circuit and have no effect on the odd-mode circuit [4].
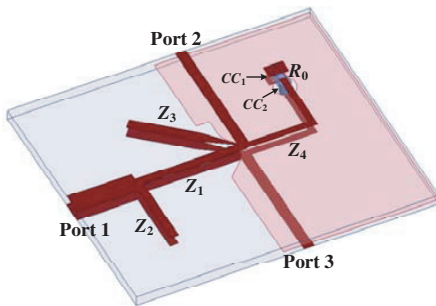
Figure 1. The circuit configuration of the proposed out-of-phase power divider.
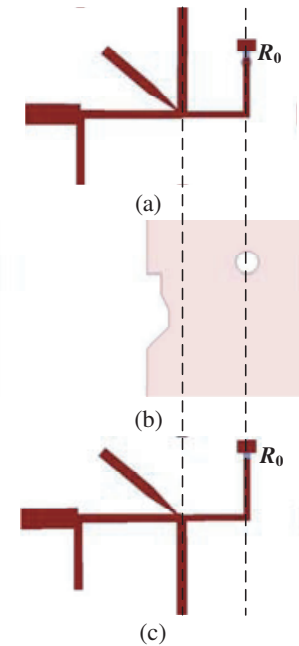
Figure 2. (a) The top layer, (b) the middle layer, and (c) the bottom layer of the proposed out-of-phase power divider.

In addition, this PD has one input port and two output ports, and the impedances of all ports are $50\,\Omega$. Output 2 is on the top layer but output 3 on the bottom layer. The phase difference between two output ports is $180°$, which is frequency independent [1] because the DSPSLs belong to the balanced transmission lines.

Furthermore, two DSPSLs Z_2 and Z_3 are used to suppress the signals at frequencies f_2 and f_3. The isolation network, which consists of the DSPSL Z_4 and the resistors R_0, can suppress all the even-order harmonics $2f_1$, where f_1 is the operating frequency.

The top, middle, and bottom layers are shown in Figure 2. It can be seen that the microstrip lines on the top and bottom layers are symmetrical, except the two output ports, indicating that the even- and odd-mode analytical method can be used in this paper [3–7]. There is a hole in the middle layer to ensure that the copper cylinder (CC_2) cannot be connected to the conductor.

2.1. Even-Mode Analysis

Under the even-mode excitation, the middle layer can be viewed as a magnetic wall because the signals on the top and bottom layers are identical, which results in no signal flowing through the input and DSPSLs Z_1, Z_2, and Z_3 [3–7]. Then, the even-mode sub-circuit can be obtained and depicted in Figure 3. Equation (1) should be satisfied to ensure that port 2 is matched, and we can derive

$$R_0 = \frac{Z_4^2}{Z_0}, \tag{1a}$$

$$\theta_4 = 90°. \tag{1b}$$
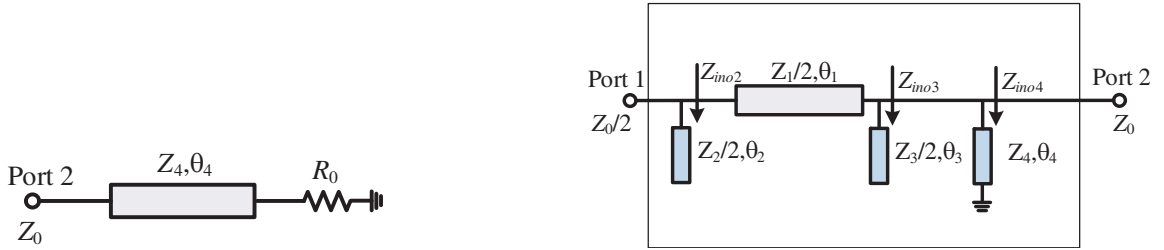
Figure 3. The even-mode sub-circuit of the out-of-phase power divider.

Figure 4. The odd-mode sub-circuit of the out-of-phase power divider.

2.2. Odd-Mode Analysis

When the odd-mode signal is excited, the middle layer can be viewed as the electrical wall for the reason that the signals on the top and bottom layer are out-of-phase [3–7]. Hence, one side of the DSPSL Z_4 is shorted, and two resistors can be omitted because CC_2 is connected to the ground [4]. The source impedances, Z_1, Z_2, and Z_3 are all half of the original values, while the characteristic impedance of DSPSL Z_4 remains the same. Then, we can obtain the odd-mode sub-circuit, which is given in Figure 4.

According to the transmission-line theory, $ABCD$ parameters in the dashed box from port 1 to port 2 can be calculated as:

$$\begin{bmatrix} A_o & B_o \\ C_o & D_o \end{bmatrix} = \begin{bmatrix} 1 & 0 \\ \dfrac{1}{Z_{ino2}} & 1 \end{bmatrix} \begin{bmatrix} \cos\theta_1 & j\dfrac{Z_1}{2}\sin\theta_1 \\ j\dfrac{2}{Z_1}\sin\theta_1 & \cos\theta_1 \end{bmatrix} \begin{bmatrix} 1 & 0 \\ \dfrac{1}{Z_{ino3}} & 1 \end{bmatrix} \begin{bmatrix} 1 & 0 \\ \dfrac{1}{Z_{ino4}} & 1 \end{bmatrix}, \tag{2}$$

where

$$Z_{ino2} = \frac{Z_2}{j2\tan\theta_2}, \tag{3a}$$

$$Z_{ino3} = \frac{Z_3}{j2\tan\theta_3}. \tag{3b}$$

$$Z_{ino4} = jZ_4\tan\theta_4. \tag{3c}$$

To ensure that port 1 is matched, we can obtain that

$$\frac{Z_0}{2} = \frac{A_o Z_o + B_o}{C_o Z_o + D_o}. \tag{4}$$

After combining Equations (1b), (2), (3) and (4), the impedances of DSPSLs Z_1, Z_2 can be calculated and listed as follows:

$$Z_1 = \frac{4Z_0^2 Z_3 \tan\theta_3 + Z_0 Z_3\sqrt{-2Z_3^2 + 2Z_3^2 \tan^2\theta_1 + 8Z_0^2 \tan^2\theta_3 + 8Z_0^2 \tan^2\theta_1 \tan^2\theta_3}}{Z_3^2 \tan\theta_1 + 4Z_0^2 \tan\theta_1 \tan^2\theta_3}, \tag{5a}$$

$$Z_2 = \frac{Z_1 Z_3 \tan\theta_1 \tan\theta_2}{2Z_1 \tan\theta_1 \tan\theta_3 - Z_3}. \tag{5b}$$

2.3. Harmonic Suppression Discussion

Since the DSPSLs Z_2 and Z_3 are used for the transmission suppression at f_2 and f_3, the corresponding electrical lengths should be $90°$ at these two frequencies. Then, the electrical lengths θ_2 and θ_3 at the operating frequency f_1 should be

$$\theta_2 = 90° \cdot \frac{f_1}{f_2}, \tag{6a}$$

$$\theta_3 = 90° \cdot \frac{f_1}{f_3}. \tag{6b}$$

It is worth noting that the electrical length θ_4 is $n \cdot 180°$ at even-order harmonic $2n \cdot f_1$, indicating that the input signal cannot be transmitted to the output because port 2 is shorted.

2.4. Scattering Parameters of the Proposed PD

The circuit theory based on the even- and odd-mode analytical method has been derived in Sections 2.1, and 2.2. Now, the scattering parameters of this proposed circuit structure is given.

First, $ABCD$ matrix of the even-mode sub-circuit in Figure 3 is calculated in Equation (7), and the odd-mode $ABCD$ parameters is obtained in Equation (2),

$$\begin{bmatrix} A_e & B_e \\ C_e & D_e \end{bmatrix} = \begin{bmatrix} \cos\theta_4 & jZ_4 \sin\theta_4 \\ j\dfrac{1}{Z_4}\sin\theta_4 & \cos\theta_4 \end{bmatrix}. \tag{7}$$

According to the matrix transformation between $ABCD$ parameters and scattering parameters [24], we can derive that

$$S_{11o} = \frac{2A_o + 2B_o/Z_0 - C_o Z_0 - D_o}{2A_o + 2B_o/Z_0 + C_o Z_0 + D_o} \tag{8a}$$

$$S_{21o} = \frac{2\sqrt{2}}{2A_o + 2B_o/Z_0 + C_o Z_0 + D_o} \tag{8b}$$

$$S_{22o} = \frac{-2A_o + 2B_o/Z_0 - C_o Z_0 + D_o}{2A_o + 2B_o/Z_0 + C_o Z_0 + D_o} \tag{8c}$$

$$S_{22e} = \frac{A_e R_0 + B_e - C_e R_0 Z_0 - D_e Z_0}{A_e R_0 + B_e + C_e R_0 Z_0 + D_e Z_0} \tag{8d}$$

Finally, the scattering parameters of this proposed PD can be derived [3] after combining Equations (2), (7), (8), and (9).

$$S_{11} = S_{11o} \tag{9a}$$

$$S_{21} = \frac{S_{21o}}{\sqrt{2}} \tag{9b}$$

$$S_{22} = \frac{S_{22o} + S_{22e}}{2} \tag{9c}$$

$$S_{23} = \frac{S_{22o} - S_{22e}}{2} \tag{9d}$$

3. PARAMETER ANALYSIS OF THE PROPOSED PD

It can be seen that the electrical lengths θ_2 and θ_3 can be determined according to Equation (6) when two suppressed frequencies f_2 and f_3 are known. In addition, the circuit parameters Z_1, Z_2, and R_0 can be obtained when θ_1, Z_3, and Z_4 are decided according to Equations (1) and (5). Since the transmission lines Z_i ($i = 1, 2$, and 3) belong to the DSPSLs, their impedance ranges should be from $40\,\Omega$ to $260\,\Omega$, and the impedance range of transmission line Z_4 is from $20\,\Omega$ to $130\,\Omega$ [5].

Additionally, the effect of the impedances Z_3 and Z_4 on the circuit scattering parameters need to be discussed in this section, and the operating frequency f_1 is chosen to be $0.92\,\text{GHz}$.

3.1. Discussion about the Impedance Z_3

Impedance Z_3 is chosen to be $50\,\Omega$, $60\,\Omega$, and $70\,\Omega$ as **Cases 1–3**, whereas the electrical length θ_1 is $40°$; the impedance Z_4 is equal to $50\,\Omega$; the first (second) suppressed frequency is $f_2 = 1.4\,\text{GHz}$ ($f_3 = 1.9\,\text{GHz}$). Then the electrical lengths of DSPSLs Z_2 and Z_3 can be calculated as $\theta_2 = 59.1429°$, and $\theta_3 = 43.5789°$ according to Equation (6). The grounded resistor is $R_0 = 50\,\Omega$ according to Equation (1a). Besides, the impedances Z_1 (Z_2) can be obtained as $93.2682\,\Omega$, $101.6540\,\Omega$, and $106.8655\,\Omega$ ($66.1921\,\Omega$, $83.7029\,\Omega$, and $104.3706\,\Omega$) for **Cases 1–3** by using Equation (5). Finally, the ideal scattering parameters, which are obtained by using the Advanced Design system (ADS) from Keysight Technologies, are plotted in Figure 5.
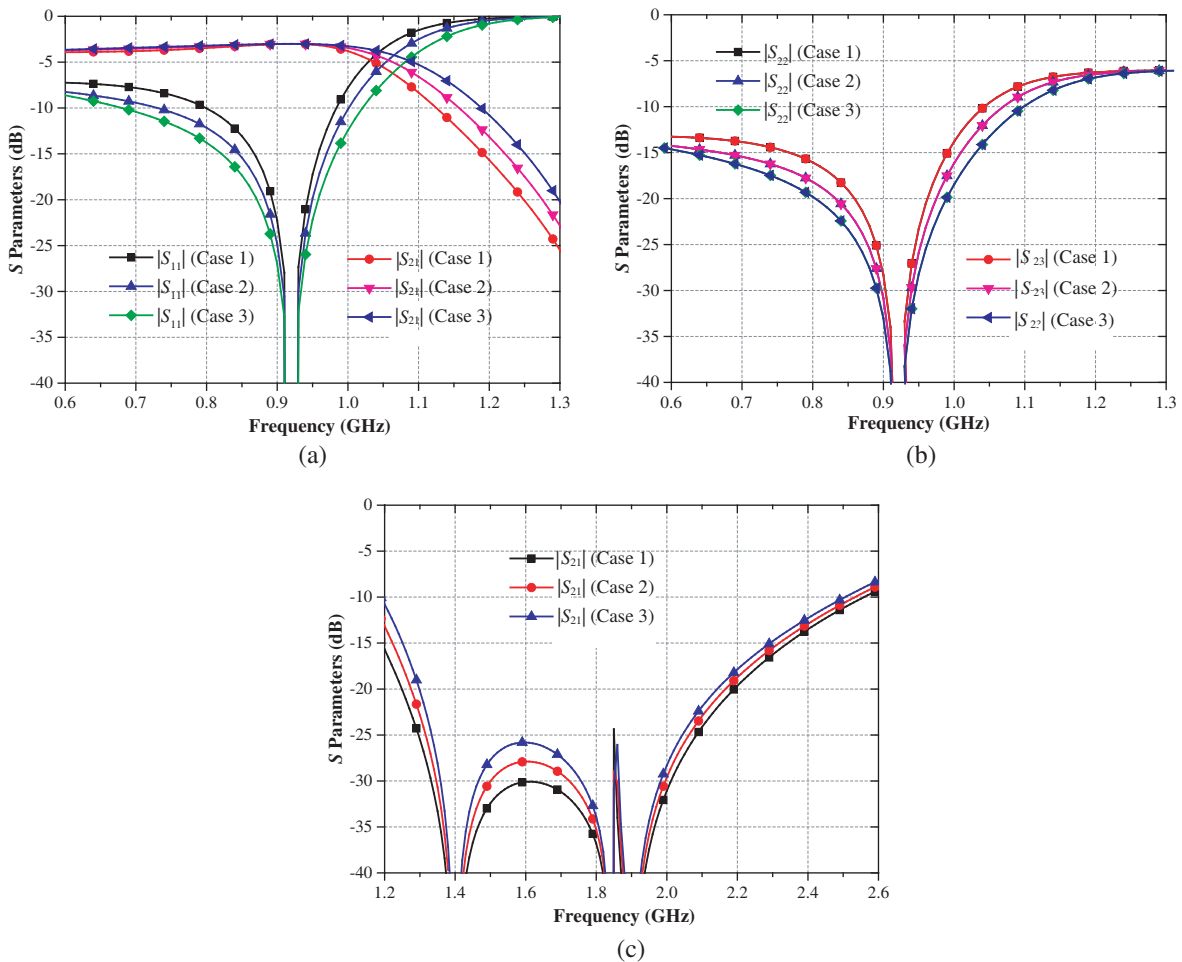
Figure 5. The magnitudes of (a) $|S_{11}|$, $|S_{21}|$ from 0.6 GHz to 1.3 GHz, (b) $|S_{22}|$, $|S_{23}|$ from 0.6 GHz to 1.3 GHz, and (c) $|S_{21}|$ from 1.2 GHz to 2.6 GHz for **Cases 1–3**.
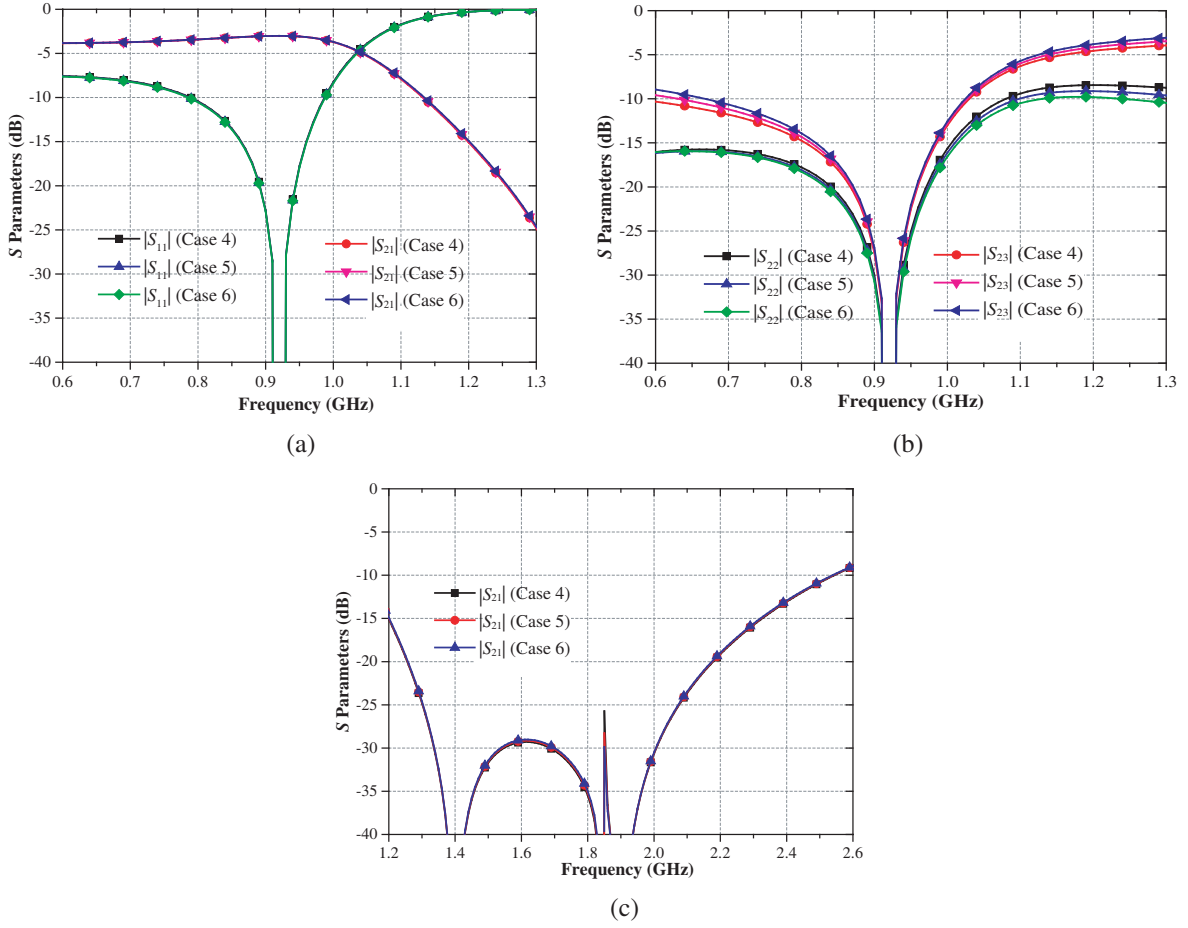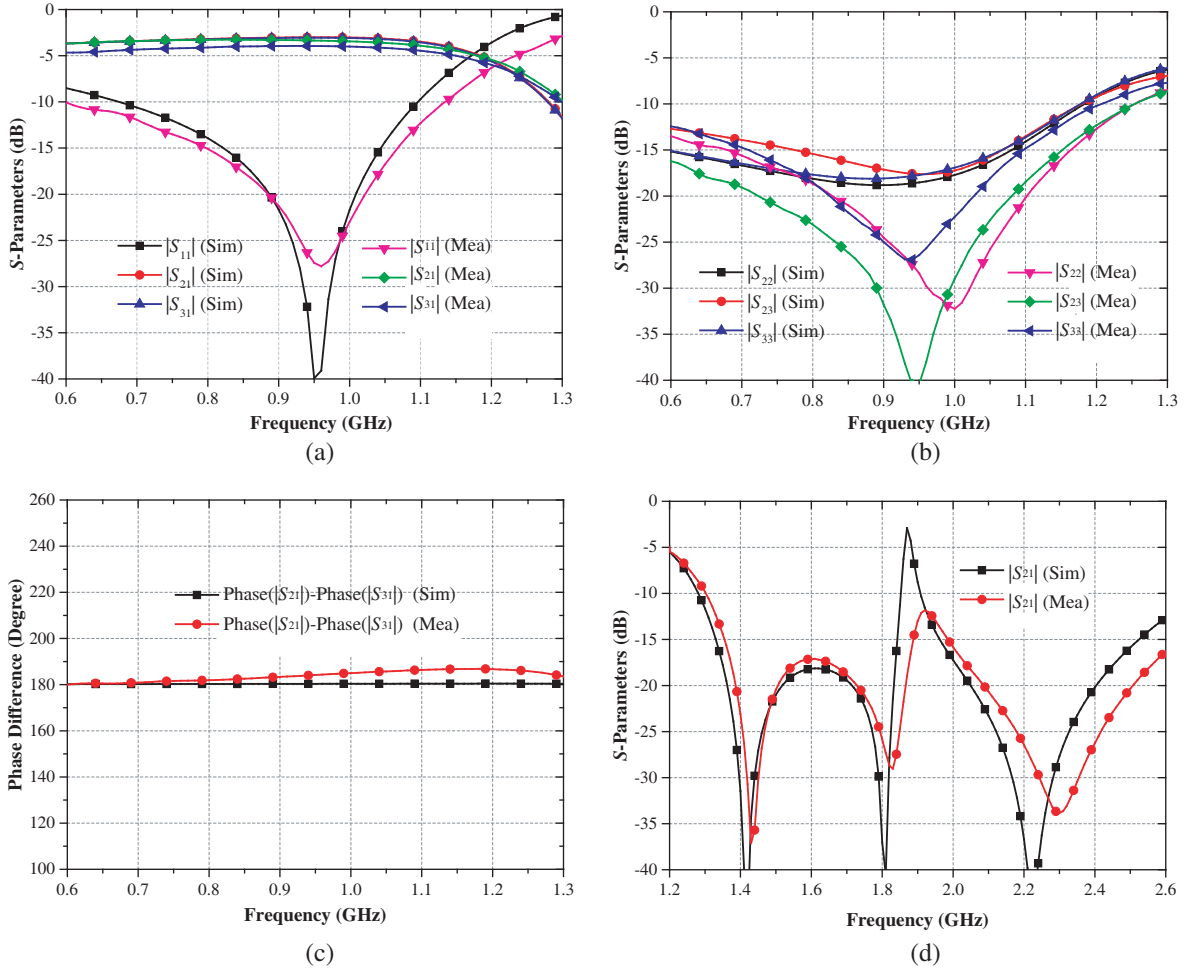
Figure 6. The magnitudes of (a) $|S_{11}|$, $|S_{21}|$ from 0.6 GHz to 1.3 GHz, (b) $|S_{22}|$, $|S_{23}|$ from 0.6 GHz to 1.3 GHz, and (c) $|S_{21}|$ from 1.2 GHz to 2.6 GHz under **Cases 4–6**.
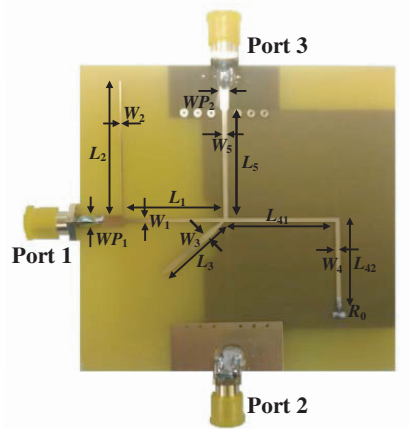
Figure 7. Bottom view of the fabricated out-of-phase PD.

It can be seen that with the increase of the impedance Z_3, the relative operating bandwidths in terms of $|S_{11}|$, $|S_{21}|$, $|S_{22}|$, and $|S_{23}|$ also increase as shown in Figures 5(a) and (b). The scattering parameters $|S_{11}|$, $|S_{22}|$, and $|S_{23}|$ are all below -40 dB, indicating the good ports matching and outputs isolation.

Figure 8. The magnitudes of (a) $|S_{11}|$, $|S_{21}|$, $|S_{31}|$ from 0.6 GHz to 1.3 GHz, (b) $|S_{22}|$, $|S_{23}|$, $|S_{33}|$ from 0.6 GHz to 1.3 GHz, (c) the phase difference from 0.6 GHz to 1.3 GHz, and (d) $|S_{21}|$ from 1.2 GHz to 2.6 GHz.

The transmission coefficient $|S_{21}|$ are all less than -40 dB at 1.4 GHz, 1.84 GHz as well as 1.9 GHz, which means that the PD realizes the transmission suppression at f_2, f_3, and $2f_1$. However, the inhibition ability from 1.2 GHz to 2.6 GHz weakens with the increase of the impedance Z_3 as shown in Figure 5(c).

3.2. Discussion about the Impedance Z_4

In this section, impedance Z_4 is chosen to be 80 Ω, 90 Ω, and 100 Ω as **Cases 4–6**, and the impedance Z_3 is 50 Ω. The electrical length θ_1 and two suppressed frequencies (f_2 and f_3) keep identical to those in **Cases 1–3**. The grounded resistors R_0 are 128 Ω, 162 Ω, and 200 Ω, respectively, for **Cases 4–6**. Since only resistor R_0 is decided by Z_4, other circuit parameters keep the same, and they are $Z_1 = 93.2682$ Ω, $Z_2 = 66.1921$ Ω, $\theta_2 = 59.1429°$, and $\theta_3 = 43.5789°$.

Finally, the calculated scattering parameters ($|S_{11}|$, $|S_{21}|$, $|S_{22}|$, and $|S_{23}|$) obtained by using the ADS are depicted in Figure 6. It can be observed that the scattering parameters change a little with the increase of the impedance Z_4, indicating that the impedance Z_4 can be chosen arbitrarily between 20 Ω and 120 Ω.

4. MEASUREMENT AND DISCUSSION

To verify the design theory in Section 2, a practical three-layer out-of-phase PD operating at 0.92 GHz for RFID application is designed and fabricated on an F4B substrate, of which the dielectric constant is 4.4, and thickness is 1.1 mm.

The source- and load-impedances are both 50 Ω, and the first (second) suppressed frequency is $f_2 = 1.4$ GHz ($f_3 = 2.2$ GHz). Other circuit parameters can be chosen and calculated as: $Z_1 = 99.9324\,\Omega$, $\theta_1 = 45°$, $Z_2 = 180.5303\,\Omega$, $\theta_2 = 59.1429°$, $Z_3 = 80\,\Omega$, $\theta_3 = 37.6364°$, $Z_4 = 80\,\Omega$, $\theta_4 = 90°$, and $R_0 = 50\,\Omega$. The bottom layer of the fabricated PD is shown in Figure 7, and the final dimensions (units: mm) are: $WP_1 = 2.61$, $WP_2 = 1.90$, $W_1 = 0.96$, $L_1 = 22.24$, $W_2 = 0.27$, $L_2 = 30.23$, $W_3 = 1.36$, $L_3 = 10.83$, $W_4 = 0.95$, $L_{41} = 24.53$, $L_{42} = 20.69$, $W_5 = 0.95$, and $L_5 = 24.05$.

The simulated and measured scattering parameters are compared and plotted in Figure 8. Notably, the circuit is simulated by using the high frequency structural simulator (HFSS) from Ansys and measured by using the Network Analyzer N5230A from Keysight Technologies. From Figure 8(a), we can see that the measured (simulated) transmission coefficients $|S_{21}|$ and $|S_{31}|$ are -3.32 dB and -3.95 dB (-3.01 dB, and -3.06 dB) at 0.92 GHz, indicating the equal power division.

In addition, the measured reflection coefficients ($|S_{11}|$, $|S_{22}|$, and $|S_{33}|$) as well as the outputs isolation ($|S_{23}|$) are all blow -23 dB at the operating frequency in Figure 8(b), which means that this PD features good ports matching and high outputs isolation.

Furthermore, the measured phase difference between two outputs is 183.7°, and the simulated phase difference is 180.3° in Figure 8(c). Finally, the transmission coefficient $|S_{21}|$ is less than -23 dB (-26 dB) at 1.4 GHz (2.2 GHz) and less than -27 dB at 1.84 GHz in Figure 8(d), which means that this PD can realize the transmission suppression at two arbitrary frequencies and even-order harmonics. The consistency between the simulated and measured results verifies the design theory.

5. CONCLUSION

A three-layer circuit structure is proposed to design an equal out-of-phase PD with harmonic suppression. This proposed PD, which consists of four DSPSLs, one middle conductor, and two grounded resistors, is analyzed based on the traditional even- and odd-mode methods, and the closed-form design equations are derived. Moreover, the parameter analysis in terms of impedance Z_3 and Z_4 is also discussed. Finally, a practical PD operating at 0.92 GHz for RFID application is designed and fabricated to verify that this PD can realize the suppression at two arbitrary frequencies and even-order harmonics.

ACKNOWLEDGMENT

REFERENCES

1. Chen, J.-X., C. H. K. Chin, K. W. Lau, and Q. Xue, "180° out-of-phase power divider based on double-sided parallel striplines," *Electron. Lett.*, Vol. 42, No. 21, 1229–1230, Oct. 2006.
2. Chen, J.-X., Z.-H. Bao, and Q. Xue, "Analysis and design of out-of-phase power divider with arbitrary division ratio," *IET Microw. Antennas Propag.*, Vol. 4, No. 9, 1370–1376, Sep. 2010.
3. Dai, G. L., X.-C. Wei, E.-P. Li, and M.-Y. Xia, "Novel dual-band out-of-phase power divider with high power-handling capability," *IEEE Trans. Microw. Theory Tech.*, Vol. 60, No. 8, 2403–2409, Aug. 2012.
4. Lu, Y. L., G.-L. Dai, X. Wei, and E. Li, "A broadband out-of-phase power divider for high power applications using through ground via (TGV)," *Progress In Electromagnetics Research*, Vol. 137, 653–667, 2013.

5. Zhang, W., Z. Ning, Y. Wu, C. Yu, S. Li, and Y. Liu, "Dual-band out-of-phase power divider with impedance transformation and wide frequency ratio," *IEEE Microw. Wirel. Compon. Lett.*, Vol. 25, No. 12, 787–789, Dec. 2015.

6. Bei, L., S. Zhang, and K. Huang, "Complex impedance-transformation out-of-phase power divider with high power-handling capability," *Progress In Electromagnetics Research Letters*, Vol. 53, 13–19, 2015.

7. Bei, L., R. Bao, L. Chen, C. Tian, X. Zhang, W. Ji, and K. Huang, "Out-of-phase power divider with complex impedance transformation based on miniaturized isolation network," *Electromagnetics*, Vol. 37, No. 3, 139–149, 2017.

8. Yi, K.-H. and B. Kang, "Modified Wilkinson power divider for nth harmonic suppression," *IEEE Microw. Wirel. Compon. Lett.*, Vol. 13, No. 5, 178–180, May 2013.

9. Xu, K., J. Shi, L. Lin, and J.-X. Chen, "A balanced-to-unbalanced microstrip power divider with filtering function," *IEEE Trans. Microw. Theory Tech.*, Vol. 63, No. 8, 2561–2569, Aug. 2015.

10. Chao, S.-F. and W.-C. Lin, "Filtering power divider with good isolation performance," *Electron. Lett.*, Vol. 50, No. 11, 815–817, May 2014.

11. Zhang, J., L. Li, J. Gu, and X. Sun, "Compact and harmonic suppression Wilkinson power divider with short circuit anti-coupled line," *IEEE Microw. Wirel. Compon. Lett.*, Vol. 17, No. 9, 661–663, Sep. 2007.

12. Wang, K. X., X. Y. Zhang, and B.-J. Hu, "Gysel power divider with arbitrary power ratios and filtering responses using coupling structure," *IEEE Trans. Microw. Theory Tech.*, Vol. 62, No. 3, 431–440, Mar. 2014.

13. Zhang, B. and Y. Liu, "Wideband filtering power divider with high selectivity," *Electron. Lett.*, Vol. 51, No. 23, 1950–1952, Nov. 2015.

14. Mirzavand, R., M. M. Honari, A. Abdipour, and G. Moradi, "Compact microstrip Wilkinson power dividers with harmonic suppression and arbitrary power division ratios," *IEEE Trans. Microw. Theory Tech.*, Vol. 61, No. 1, 61–68, Jan. 2013.

15. Woo, D.-J. and T.-K. Lee, "Suppression of harmonics in Wilkinson power divider using dual-band rejection by asymmetric DGS," *IEEE Trans. Microw. Theory Tech.*, Vol. 53, No. 6, 2139–2144, Jun. 2005.

16. Yang, J., C. Gu, and W. Wu, "Design of novel compact coupled microstrip power divider with harmonic suppression," *IEEE Microw. Wirel. Compon. Lett.*, Vol. 18, No. 9, 572–574, Sep. 2008.

17. Lin, C.-M., H.-H. Su, J.-C. Chiu, and Y.-H. Wang, "Wilkinson power divider using microstrip EBG cells for the suppression of harmonics," *IEEE Microw. Wirel. Compon. Lett.*, Vol. 17, No. 10, 700–702, Oct. 2007.

18. Zhang, F. and C. F. Li, "Power divider with microstrip electromagnetic bandgap element for miniaturisation and harmonic rejection," *Electron. Lett.*, Vol. 44, No. 6, 422–424, Mar. 2008.

19. Ren, X., K. Song, B. Hu, and Q. Chen, "Compact filtering power divider with good frequency selectivity and wide stopband based on composite right-/left-handed transmission lines," *Microw. Opt. Technol. Lett.*, Vol. 56, No. 9, 2122–2125, Sep. 2014.

20. Wang, J., J. Ni, Y.-X. Guo, and D. Fang, "Miniaturized microstrip Wilkinson power divider with harmonic suppression," *IEEE Microw. Wirel. Compon. Lett.*, Vol. 19, No. 7, 440–442, Jul. 2009.

21. Zhang, Z., Y.-C. Jiao, and Z.-B. Weng, "Design of 2.4 GHz power divider with harmonic suppression," *Electron. Lett.*, Vol. 48, No. 12, 705–707, Jun. 2012.

22. Chen, C.-F., T.-Y. Huang, C.-C. Chen, W.-R. Liu, T.-M. Shen, and R.-B. Wu, "A compact filtering rat-race coupler using dual-mode stub-loaded resonators," *IMS 2012-2012 IEEE MTT-S International Microwave Symposium*, 3 pages, Montreal, QC, Canada, Jun. 17–22, 2012.

23. Wang, K.-X., X. Y. Zhang, S. Y. Zheng, and Q. Xue, "Compact filtering rat-race hybrid with wide stopband," *IEEE Trans. Microw. Theory Tech.*, Vol. 63, No. 8, 2550–2560, Aug. 2015.

24. Ahn, H.-R. and B. Kim, "Toward integrated circuit size reduction," *IEEE Microw. Mag.*, Vol. 9, No. 1, 65–75, Feb. 2008.